

Cp* versus Bis-carbonyl Iridium Precursors as CH Oxidation Precatalysts

Daria L. Huang,[§] David J. Vinyard,[§] James D. Blakemore,^{†,§} Sara M. Hashmi,[‡] and Robert H. Crabtree^{*,§}

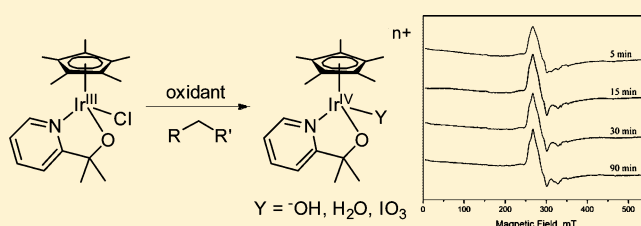
[†]Department of Chemistry, University of Kansas, 1251 Wescoe Hall Drive, 2010 Malott Hall, Lawrence, Kansas 66045, United States

[‡]Department of Chemical and Environmental Engineering, Yale University, 9 Hillhouse Avenue, New Haven, Connecticut 06520, United States

[§]Department of Chemistry, Yale University, 225 Prospect Street, New Haven, Connecticut 06520, United States

S Supporting Information

ABSTRACT: We previously reported a dimeric Ir^{IV}-oxo species as the active water oxidation catalyst formed from a Cp*Ir(pyalc)Cl {pyalc = 2-(2'-pyridyl)-2-propanoate} precursor, where the Cp* is lost to oxidative degradation during catalyst activation; this system can also oxidize unactivated CH bonds. We now show that the same Cp*Ir(pyalc)Cl precursor leads to two distinct active catalysts for CH oxidation. In the presence of external CH substrate, the Cp* remains ligated to the Ir center during catalysis; the active species—likely a high-valent Cp*Ir(pyalc) species—will oxidize the substrate instead of its own Cp*. If there is no external CH substrate in the reaction mixture, the Cp* will be oxidized and lost, and the active species is then an iridium- μ -oxo dimer. Additionally, the recently reported Ir(CO)₂(pyalc) water oxidation precatalyst is now found to be an efficient, stereoretentive CH oxidation precursor. We compare the reactivity of Ir(CO)₂(pyalc) and Cp*Ir(pyalc)Cl precursors and show that both can lose their placeholder ligands, CO or Cp*, to form substantially similar dimeric Ir^{IV}-oxo catalyst resting states. The more efficient activation of the bis-carbonyl precursor makes it less inhibited by obligatory byproducts formed from Cp* degradation, and therefore the dicarbonyl is our preferred precatalyst for oxidation catalysis.



INTRODUCTION

The selective activation of CH bonds is a highly desirable reaction that has attracted great interest for many years.^{1–7} CH oxidation is an especially valuable version, as it is highly relevant to selective chemical synthetic processes for late-stage functionalization of organic molecules.^{8–14} Several metalloproteins are known to carry out oxidation reactions in nature through metal-oxo species, most commonly using high-valent first-row transition metals.^{15–20} These metalloproteins generally operate via intermediate radicals.^{21–25} In contrast, many synthetic complexes, including those discussed here, have metal-oxo intermediates, where an oxene-like insertion permits a stereoretentive reaction.^{26,27}

In previous reports, we and others have demonstrated that Cp*Ir compounds, such as Cp*Ir(pyalc)Cl (Figure 1, 1), are competent CH oxidation precatalysts.^{28–33} Later reports proposed an Ir^{IV}-oxo dimer as the active species for both water oxidation (WO) and CH oxidation catalysis, following oxidative degradation of the Cp* ligand to primarily give AcOH.³⁴ Despite extensive work on this system, the active form of the catalyst is not yet fully defined, as it cannot be crystallized for structural study. Recent spectroscopic and HEXS data suggest a mono- μ -oxo di-iridium structure as the preferred active species (2).³⁵ A number of stereoisomers may well be present, accounting for its reluctance to crystallize.^{36,37}

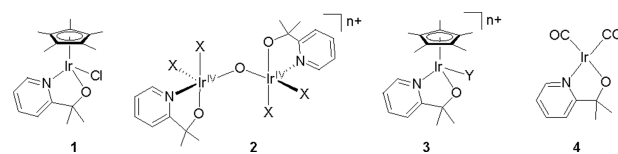
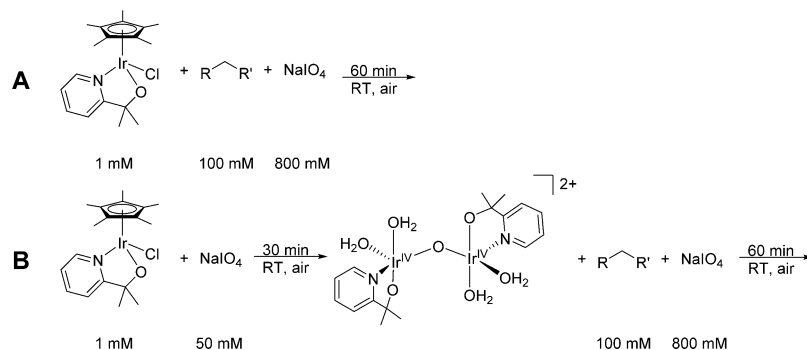


Figure 1. Cp*Ir^{III}(pyalc)Cl (1), Ir^{IV}-oxo dimer (2), monomeric Cp*Ir^{IV}(pyalc) reaction intermediate (3), and the Ir^I(CO)₂(pyalc) (4). Species 2 is thought to be a mixture of stereoisomers with X possibly being H₂O, acetate, or iodate under turnover conditions. Species 3 is thought to be a resting state in the CH oxidation catalysis with Y possibly being H₂O, ⁻OH, acetate, or iodate under turnover conditions.

Although Cp* is oxidatively degraded under catalytic conditions for WO,^{34,38–40} we were curious to see if rapid degradation would still occur if more reactive CH substrates were also present in the reaction mixture. We now report that the Cp* complex 1 can retain its Cp* group under CH oxidation conditions, and the catalyst progresses to 2 only when no CH substrate is present. We have identified a Cp*Ir^{IV}(pyalc) species (3) as a long-lived resting state in CH

Special Issue: Hydrocarbon Chemistry: Activation and Beyond

Received: June 28, 2016

Scheme 1. Different Reaction Protocols for CH Oxidation Catalysis^a

^aProtocol A has no preactivation phase, and all reagents are added at the same time, while protocol B involves a pre-activation phase that deliberately removes the Cp* with oxidant prior to adding the CH substrate and more oxidant.

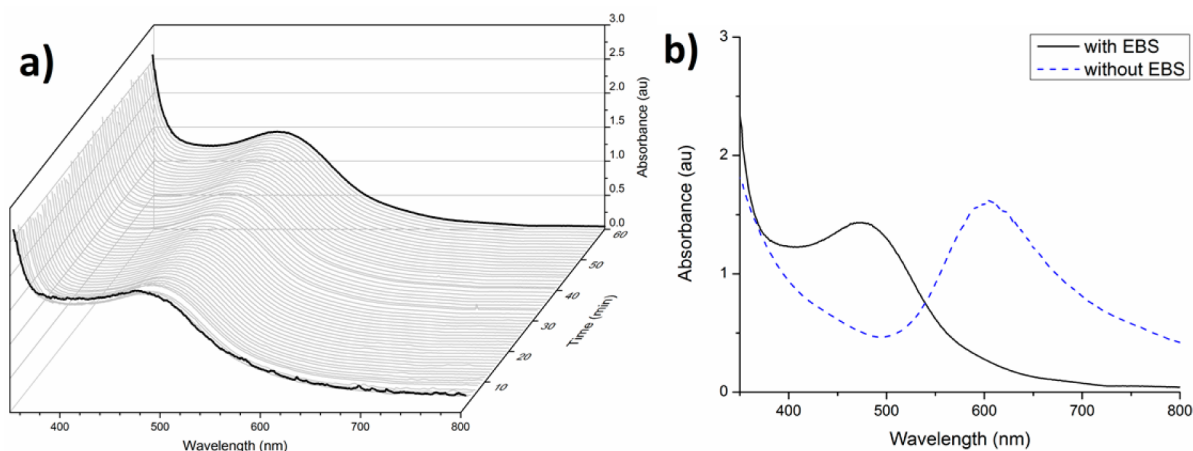


Figure 2. (a) UV-vis spectra over 1 h of a solution of **1** (1 mM) in the presence of 100 mM sodium 4-ethylbenzenesulfonate (EBS) as CH substrate and 400 mM NaIO₄ as oxidant. (b) UV-vis spectra of a solution of **1** (1 mM) after addition to a solution of NaIO₄ and EBS (black line) versus a 1 mM solution of **1** in the presence of 400 mM NaIO₄ alone (blue dashed line).

oxidation catalysis, suggesting that the active CH oxidation species is a high-valent Ir(pyalc) species with the Cp* still ligated to the metal center. The Cp*Ir(pyalc) active species will oxidize the external CH substrate rather than its own Cp* ligand. A Cp*Ir^{IV} species has previously been suggested as a catalytic intermediate in CH activation catalysis,^{41,42} but to the best of our knowledge this is the first report in which we identify a Cp*Ir^{IV} resting state in solution-state reaction conditions by means of a number of spectroscopic techniques.

Recently we reported a new Ir bis-carbonyl precursor (**4**) as an improvement over **1** for WO catalysis.⁴³ Here, we now show that **4** is also a competent CH oxidation precatalyst. Both **1** and **4** likely form substantially similar species of general type **2** after their placeholder ligands, CO and Cp*, respectively, undergo oxidative degradation, but we see faster activation of the dicarbonyl precatalyst. Moreover, **4**, lacking the Cp* ligand, does not form complicating byproducts, such as AcOH, iodate, and methanol, during the Cp* degradation process. We show that this change of the placeholder ligands makes the bis-carbonyl precatalyst (**4**) more rapidly activating and efficient at CH oxidation, making it the preferred precursor over **1**.

Importantly, the dicarbonyl precursor does not give AcOH as a byproduct of activation, and thus the Ir-oxo species **2** produced in the activation process lacks this potential ligand. We now find that **4** requires the addition of AcOH to give significant yields in CH oxidation, thus indicating that AcOH is

a needed coligand for **2** to become catalytically active for CH oxidation. This emphasizes the importance of acetic acid as an *in situ* ligand for promoting catalysis for **2**, something we were able to discover and study only by using a precursor that lacks Cp* ligands and thus lacks the AcOH degradation product.

RESULTS

Characterization of High-Valent Monomeric Cp*Ir Species. In initial work by Zhou et al. with the Cp*Ir series as CH oxidation precatalysts,^{28,30} the precatalyst was always added simultaneously with the oxidant and substrate (Scheme 1, protocol A); no steps were taken to preactivate the Cp*Ir precatalyst to remove the Cp* (protocol B). This Cp* degradation process was reported only after the work by Zhou et al. and therefore was not taken into account by them. We could not then be sure if the active species in the CH oxidation reaction was a mononuclear derivative of **1** with the Cp* still present or whether the Cp* was degraded preferentially over the CH substrate and that **2** oxidized the CH bonds. The mononuclear catalytic species has been alluded to before: Templeton and co-workers have isolated and characterized a Cp*Ir compound that retains its placeholder ligand and is still able to perform stoichiometric oxidation reactions.^{41,44,45} They propose the active species as a high-valent mononuclear Cp*Ir species. In the present paper, we report several pieces of evidence that indicate that for CH

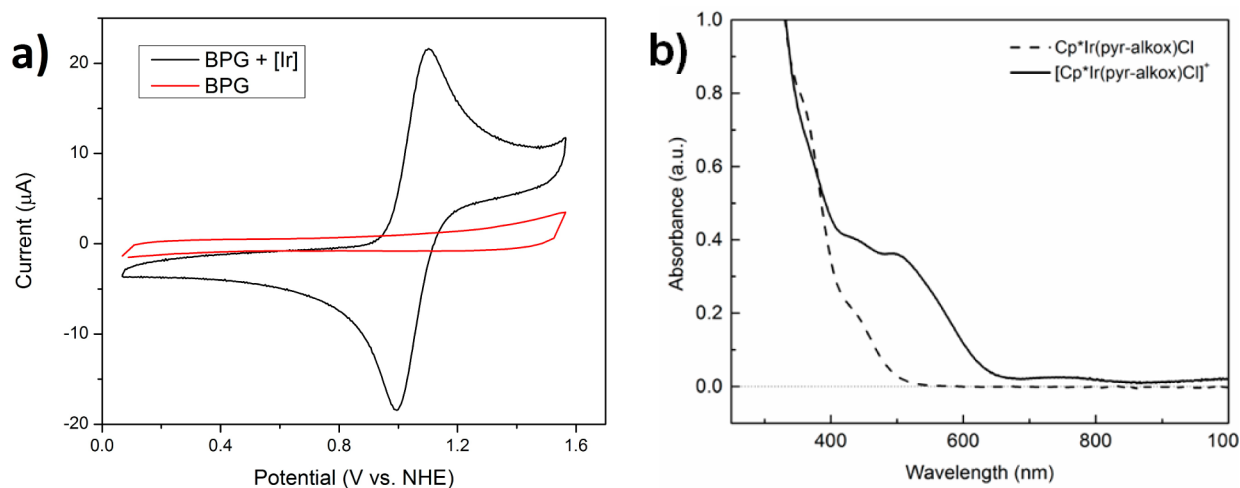


Figure 3. (a) Cyclic voltammogram of 1 mM **1** in MeCN with 0.1 M $\text{Bu}_4\text{N}^+\text{PF}_6^-$ as the supporting electrolyte. Scan rate: 200 mV/s with basal plane graphite (BPG) working electrode. (b) UV-vis spectra of **1** before and after applying a 1 V potential for 30 min. More information can be found in the [Experimental Section](#).

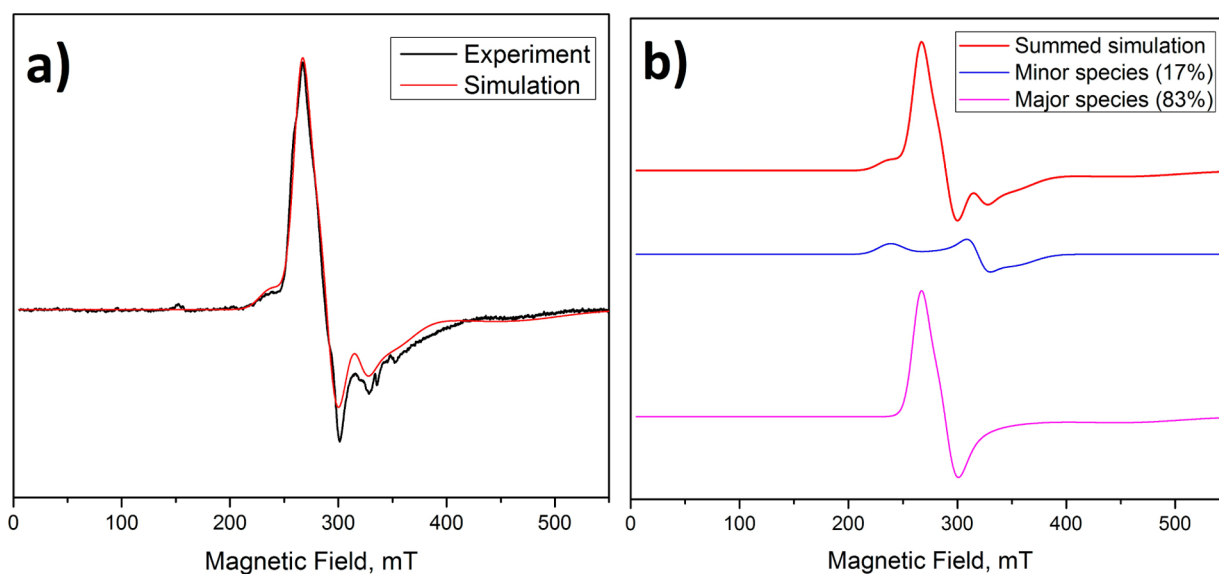


Figure 4. X-band EPR spectra. (a) **1** in a representative CH oxidation reaction: 50 nmol (500 μM) of **1** is added to 250 mM NaIO_4 and 50 mM THF in water (black line). The reaction is allowed to proceed for 5 min prior to sparging and freezing. The simulation of the spectra is in red. (b) Breakdown of the two simulation components.

oxidation reactions with precursor **1** the Cp^* remains ligated to the metal center, as suggested by our EPR and UV-vis observations, which suggest we have a mononuclear $\text{Cp}^*\text{Ir}^{\text{IV}}$ resting state of type **3**. In contrast, dicarbonyl **4** rapidly loses the placeholder ligand and forms a μ -oxo species as a catalytic resting state, as shown later in this paper.

Under normal CH oxidation conditions, where the catalyst is added to the substrate and oxidant without any preactivation of the compound (protocol A), the reaction retains its orange color and absorbs strongly at 485 nm (Figure 2a). This band persists even after the CH oxidation reaction is completed and remains stable in solution for more than 3 days. The ^1H NMR spectrum of the reaction mixture shows that the Cp^* signal remains, with no trace of acetic acid, a major byproduct of the Cp^* degradation as part of the activation process for **WO** (Figure S1). In contrast, following protocol B with the deliberate removal of the Cp^* in a preactivation phase in contact with oxidant alone to remove the Cp^* , the solution

turns blue and absorbs at 610 nm (Figure 2b). This is the procedure that Hintermair et al. use to form the Ir^{IV} -oxo dimer (**2**), with the Cp^* primarily degrading into acetic acid in the preactivation process.³⁴ Additionally, if a substrate, such as sodium benzenesulfonate, is added that lacks very easily oxidizable CH bonds, the Cp^* placeholder ligand will also be preferentially attacked and **2** will be formed (Figure S2). Therefore, for protocol A to be effective, available and very easily oxidizable CH bonds must be present in the substrate to protect the Cp^* from degradation.

This $\lambda_{\text{max}} = 485$ nm species was further investigated by electrochemistry. When a solution of **1** is scanned over a range of potentials, we see a metal-centered redox process at 1 V vs NHE with a peak-to-peak separation of 99 mV, which is consistent with a quasireversible $\text{Ir}^{\text{III/IV}}$ couple (Figure 3a). When a fixed potential of 1 V (vs NHE) is applied to a solution of **1**, a new spectral band grows in at 530 nm (Figure 3b), similar to the $\lambda_{\text{max}} = 485$ nm species produced from the

chemical oxidation of **1** (Figure 2a). The shift from 485 to 530 nm may be due to the difference in solvent, electrolyte, and pH conditions. More importantly, this species is clearly distinct from **2**, which absorbs at 610 nm, and supports the idea that, though a high-valent Ir is being formed, the Cp* remains bound to the metal center. Thomsen et al. could not fully remove the Cp* from **1** electrochemically only by applying a potential of 1.4 V vs NHE over the course of 48 h.⁴⁶ This is a promising sign that Cp*Ir compounds may be efficient electrocatalysts for CH oxidation without Cp* loss; work is ongoing in the lab to further probe this point.

An EPR spectrum of **1** in a CH oxidation reaction using protocol A gives a spectrum that appears broad and nearly axial (Figure 4a). However, simulations show that the signal is best fit when there are two unique species, both of which are rhombic (Figure 4b). The dominant species (83%) was modeled using the *g*-values 2.503, 2.293, and 1.426, and line broadening was simulated using the *g*-strain tensor [0.149 0.160 0.333]. The minor feature (17%) was modeled using the *g*-values 2.809, 2.091, and 1.877, and line broadening was simulated using the *g*-strain tensor [0.307 0.118 0.220]. Although EPR examples of Cp*Ir^{IV} species are rare, these values align with those reported by our group^{47,48} and others.^{49–52} Importantly, the presence of an EPR signal indicates that **2** is not the dominant CH oxidation species, as it is EPR silent, at least in the usual IV,IV oxidation state.³⁴ This is also a unique example of a Cp*Ir^{IV} species observed in reaction conditions, rather than oxidized by electrode or by [Ru(bipy)₃]³⁺. For the purposes of this paper, we will consider the dominant feature as the main species in the reaction.

The fact that the observed EPR signal assigned to Ir(IV) persists for over an hour of reaction time (Figure 5) is

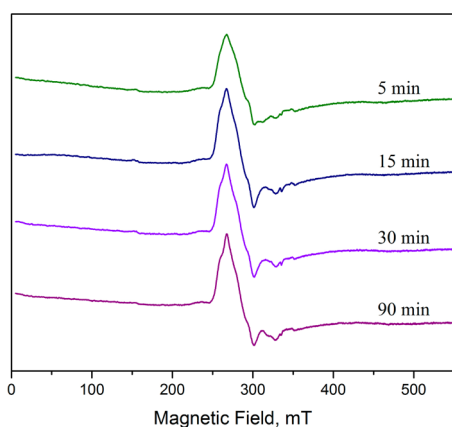


Figure 5. EPR signals recorded in a representative CH oxidation reaction over the course of 90 min.

consistent with the presence of an Ir(IV) resting state for the system. This is also consistent with the UV–vis data (Figure 2a). This resting state is likely similar in structure to **3** and is a mononuclear paramagnetic Cp*Ir^{IV} species. Additionally, the signal does not change when screening other CH substrates and solvents (Figures S3 and S4). This indicates that the proposed monomeric [Cp*Ir^{IV}(pyalc)-Y]ⁿ⁺ resting state does not have a CH substrate ligated to the metal center. The resting state is likely a precursor to the active form, possibly a high-valent Cp*Ir^V(pyalc)-oxo or -oxene, which we have not been able to characterize yet but have previously described by DFT.²⁹ The rate-determining step is likely the oxidation of **3** to

this high-valent Cp*Ir^V(pyalc)-oxo or -oxene species, which then oxidizes either the CH substrate, the Cp*, or the solvent water depending on the reaction conditions.

Given that we have two potential catalytic species (**2** or **3**) that can be derived from the precatalyst **1**, we wondered if they have the same reactivity for CH oxidation catalysis. If we follow protocol A and form the active species **3**, we find high oxidation yields for a variety of substrates, as observed by Zhou (Table 1).²⁸ However, if **1** is preactivated with 50 equiv of NaIO₄ to

Table 1. CH Oxidation Yields for Select Substrates from **1**, Following Protocol A or B^a

Entry	Substrate	Product	Yield for protocol A	Yield for protocol B
1			55%	45%
2			48%	37%

^aReaction conditions: Oxidant pre-dissolved in H₂O and added to the substrate and precatalyst **1** and allowed to stir at 25 °C for 60 min in air. Yields were determined by ¹H NMR against TMSP-*d*₄ as a standard. More information can be found in the Experimental Section.

remove the Cp* and form **2** (protocol B), we find that the addition of CH substrates and additional oxidant gives lower oxidized CH product yields. We believe that this discrepancy is due to inhibition of **2**, the Cp* degradation products; the preactivation step in protocol B requires that a significant amount of periodate be used to remove the Cp* and necessarily produces degradation byproducts AcOH and iodate, but also formic acid, methanol, and ethanol, known powerful reductants.^{38,40,46} The presence of CH oxidation byproducts from the Cp* degradation distinguishes protocols A and B; these byproducts may well inhibit CH oxidation catalysis and cause the difference in yields.

Ir(CO)₂(pyalc), **4, as an Alternative CH Oxidation Precatalyst.** Considering that the obligatory degradation products of the preactivation phase of **1** to **2**, such as methanol, ethanol, and formic acid, inhibit oxidation catalysis, we turned to a different precatalyst, which produces the same or very similar species to **2**, but with much fewer activation byproducts. The recently reported that the Ir^I(CO)₂(pyalc) precursor (**4**) was shown to be a robust WO precatalyst, in part because it activates much more quickly and easily than the analogous **1** and with no observable byproduct.⁴³ The CO ligands are lost more easily and quickly than Cp*; more importantly, **4** requires only 2 equiv of oxidant to become activated, compared with a minimum of 50 equiv for **1**. Given the success of precursor **4** as a WO precatalyst and its facile preactivation, we decided to test it for CH oxidation catalysis.

In optimizing the CH oxidation conditions for dicarbonyl **4**, we adapted what we learned from WO experiments, notably, the requirement for the presence of AcOH to stabilize the active species of type **2**. For terminal oxidants, we tested several different water-soluble and heterogeneous oxidants for the oxidation of model substrate 4-ethylbenzenesulfonate (EBS) to 4-acetophenone sulfonate (APS) (Table 2). Of the 10 oxidants tested, sodium periodate, periodic acid, and ceric ammonium nitrate (CAN) gave the highest yields. However, given the well-known difficulties⁵³ of using CAN at pH higher than 2 and its interference with UV–vis and NMR experiments, owing to its

Table 2. Screened Oxidants Using 4 as a Precatalyst for EBS Conversion to APS^a

oxidant	APS yield (%)	oxidant	APS yield (%)
NaIO ₄	78	PbO ₂	7
H ₅ IO ₆	81	H ₂ O ₂	0
CAN	91	^t BuOO ^t Bu	0
NaClO	20	LiO ₄	0
^t BuOOH	38	I ₂ O ₅	0
Oxone	11	NaIO ₃	0
KBrO ₃	10	air (control)	0

^aReaction conditions: Oxidant predissolved/mixed in H₂O and added to the substrate, dicarbonyl precatalyst 4, and AcOH and allowed to stir at 25 °C for 60 min. Yields were determined by ¹H NMR against TMSP-*d*₄ as a standard. Mass balance was >95% for all reactions. More information can be found in the [Experimental Section](#).

color and paramagnetism, we used NaIO₄ and H₅IO₆ for subsequent experiments.

Interestingly, the amount of added acetic acid seems to significantly affect the oxidation product yields ([Table 3](#)). In the

Table 3. EBS Oxidation Yields from 4 with Varying mol % of Added AcOH^a

mol % AcOH	APS yield (%)
0	14
0.5	21
1	39
5	48
50	47

^aReaction conditions: Oxidant predissolved in H₂O and added to the substrate, precatalyst 4, and AcOH and allowed to stir at 25 °C for 60 min in air. The amount of AcOH was varied between each reaction. Yields were determined by ¹H NMR against TMSP-*d*₄ as a standard. More information can be found in the [Experimental Section](#).

absence of any acetic acid, very little EBS is converted to APS. However, this does not seem to be the case because 1 degrades into nanoparticles, which was shown previously to be detrimental to oxidative catalysis.⁴³ On the CH oxidation time scale (30 min to 1 h), the Ir active species is shown to be homogeneous by dynamic light scattering (DLS) with EBS present in the reaction mixture, even if there is no acetic acid present ([Figure S6](#)). The necessity for the presence of added acetic acid for efficient CH oxidation indicates that acetic acid not only stabilizes the homogeneous species⁴³ but also acts as an *in situ* ligand for the active species and thereby promotes CH oxidation. A slight excess of AcOH is used in CH oxidation reactions using dicarbonyl 4 as a precatalyst, as AcOH can be oxidized as part of the reaction; small amounts of formate are observed in the ¹H NMR product spectra. We do not see a difference in yields if we use protocols A and B with dicarbonyl precatalyst 4; that is, there is no difference in CH oxidation product yields if we mix 4, oxidant, and CH substrate all at once or if we preactivate 4 with a small amount of oxidant and then add CH substrate and more oxidant. This is not unexpected, as previous WO work has shown that 4 loses its CO placeholder ligands and activates extremely quickly to a species similar to 2.⁴³ Precatalyst 4 likely has no other active oxidation species like the Cp*Ir precatalysts. For all CH oxidation experiments with 4, we added all reagents at once (protocol A).

In testing a variety of different substrates for CH oxidation, we find similar efficiencies between 4 and the analogous

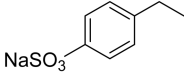
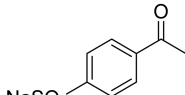
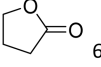
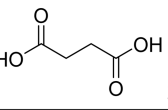
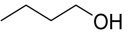
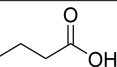
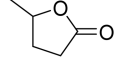
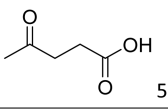
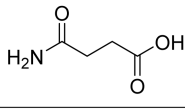
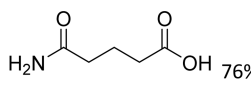
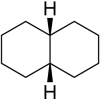
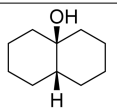
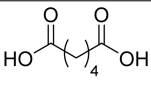
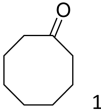
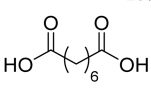
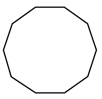
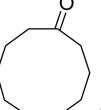
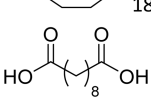
Cp*Ir(pyalc)Cl (1) for water-soluble substrates ([Table 4](#)). 4 gives high yields for heterocycles such as THF and pyrrolidine, indicating it is not poisoned by substrate binding. As in the prior work with the Cp* precursor, we checked whether these reactions were stereoretentive. Oxidation of *cis*-decalin to *cis*-decalol (entry 7) with retention of configuration indeed indicates a concerted oxidation pathway as inferred by Zhou et al.³⁰ Cycloalkanes are also efficiently oxidized to the corresponding diacid. We believe that the catalyst likely performs the initial oxidation of the cycloalkane to the corresponding ketone, and the ketone then goes through a Baeyer–Villiger oxidation to form a lactone. Subsequent lactone hydrolysis would be expected to give a hydroxy-substituted carboxylic acid, which would then undergo further oxidation to the diacid (entries 8–10), the observed final product. However, it is unclear whether the catalyst or oxidant gives the Baeyer–Villiger oxidation to form a lactone; many peracids, periodic acid included, can perform Baeyer–Villiger O atom insertion into ketones to form esters.⁵⁴ However, periodic acid cannot oxidize the cycloalkane without a catalyst, so the initial oxidation is metal-driven. The product distribution also indicates that the majority of the oxidant is being used in metal-based oxidation of the cycloalkane to the cyclic ketone.

For organic substrates as a whole, the turnover frequencies (TOFs) for 4 are generally better than those reported for 1. We believe that the greater solubility of periodic acid over sodium periodate in these organic systems may help increase yields. However, 4 gave significant yields of oxidized CH products only in a MeCN/H₂O solvent system with H₅IO₆ as an oxidant. Acetone/H₂O and ^tBuOH/H₂O solvent systems gave much lower yields, and hexafluoroisopropanol (HFIP)/H₂O did not work at all, as HFIP was immediately oxidized by H₅IO₆ even without a catalyst. This solvent sensitivity distinguishes 4 from 1, as Zhou et al. reported that 1 was an efficient precatalyst in all four solvent systems listed here. This may be because Zhou et al. had been working under the conditions of protocol A, so the active Ir species in this previous CH oxidation work still has the Cp* ligated to the metal center to form a resting state of type 3. The Cp*Ir active species may be more soluble and/or less sensitive to solvent conditions than the active species for precatalyst 4, likely an Ir-oxo dimer similar to 2, thus maintaining many open sites. However, since 4 has higher TOFs for organic substrates relative to 1, future CH oxidation work would benefit from using 4 in terms of optimizing yields.

■ CONCLUSION

We show that Ir(CO)₂(pyalc) (4) is a competent CH oxidation precatalyst able to oxidize many substrates under a variety of conditions, including the stereoretentive oxidation of *cis*-decalin to *cis*-decalol. The precatalyst requires acetic acid to efficiently oxidize CH bonds. This AcOH acts as both a stabilizing agent against nanoparticle formation and a ligand that promotes CH oxidation catalysis. In contrast, for WO, acetic acid acts only as a stabilizing agent and not a promoter ligand. We also show that the Cp*Ir(pyalc)Cl (1) precatalyst has two pathways to oxidize CH bonds. Without preactivation to remove Cp* before adding external CH substrate, the initially formed active species is a high-valent mononuclear Ir-oxo species with the Cp* still ligated to the metal center, suggested by the mononuclear Cp*Ir^{IV}(pyalc) resting state of type 3, which we have identified. If the Cp* is deliberately removed in a preactivation step, the active species is now an Ir^{IV}-oxo dimer of type 2, competent for WO and CH oxidation catalysis. A

Table 4. CH Substrates Oxidized by 4^a

Entry	Substrate	Product yield	TOF (h ⁻¹) ^b	TOF (h ⁻¹) of 1, path A
1		 78%	78	55
2		 60%  21%	81	82 (diacid only)
3		 45%	45	47 ^c
4		 24%  51%	75	62 (keto-acid only)
5		 50%	50	61
6		 76%	76	56
7		 52%	52 ^d	0.5 ^c
8		 21%	21	13 ^c
9		 15%  11%	26	1.2 ^c (only ketone)
10		 18%  10%	28	0.7 (only ketone)

^aReaction conditions: Oxidant predissolved in solvent and added to the substrate, precatalyst 4, and AcOH and allowed to stir at 25 °C for 60 min in air. Yields were determined by ¹H NMR against a standard. For entries 1–6, the solvent was H₂O, the oxidant NaIO₄, and the standard TMSP-d₄. For entries 7–10, the solvent was MeCN/H₂O (4:1), the oxidant H₃IO₆, and the standard 1,3,5-trichlorobenzene. ^bTOF is based on the oxidation of the first CH bond. ^cTOF calculated from Zhou et al.²⁸ ^dYield was determined by GC/MS according to literature procedure.³⁰ More information can be found in the Experimental Section.

species substantially similar to 2 is also formed by the activation of Ir(CO)₂(pyalc). However, because 1 requires significantly more periodate for activation to give 2, the increased amount of obligatorily coproduct, iodate, acts as an inhibitor. In the absence

of such byproducts though, 2 is an efficient CH oxidation catalyst. This is confirmed through the more easily activated 4, where minimal iodate is involved in preactivation. Given that 4 has been shown to more efficiently activate to 2 with fewer

byproducts, and therefore is more efficient for WO⁴³ and CH oxidation reactions, future experiments will examine the reactivity of Ir^{IV}-oxo dimer and will test Ir(CO)₂(pyalc) as the precursor rather than any Cp*Ir analogues. This is especially true for electrochemical studies, where byproducts must be minimized in order to prevent electrode side-reactions and inhibition.

EXPERIMENTAL SECTION

General Procedures. All organic solvents were dried using a Grubbs-type purification system. High-purity Milli-Q water was used for all aqueous experiments. All chemicals were purchased from major suppliers and used without further purification. Syntheses were performed using standard Schlenk techniques under a dry atmosphere of N₂. The 2-(2'-pyridyl)-2-propanoate (pyalc) ligand,⁵⁵ Cp*Ir^{III}(pyalc)Cl,⁵⁶ and Ir^I(CO)₂(pyalc)⁴³ were prepared according to previous literature procedures. ¹H NMR spectra were collected at room temperature on a 400 or 600 MHz Varian spectrometer and referenced to the residual solvent signal or an added standard (δ in ppm, J in Hz). Dynamic light scattering experiments were conducted based on a literature procedure.⁴³

For CH oxidation reactions: 0.2 mmol of CH substrate was dissolved with 2 μ mol (1 mol %) of precatalyst and additive (only used for precatalyst 4) in 2 mL of solvent. The oxidant (2 mmol) was predissolved or mixed in 8 mL of solvent in a separate vial. The oxidant was added to the substrate and catalyst solution to initiate the reaction and allowed to stir at 25 °C for 60 min in air. With the exception of *cis*-decalin, the reaction was stopped by taking a 1 mL aliquot and removing the solvent *in vacuo*. The resulting solids were dissolved in D₂O or DMSO-*d*₆, and yields were determined by ¹H NMR against an external standard. For *cis*-decalin, the reaction was worked up by using a literature procedure of extracting with ethyl acetate and determining yields by GC/MS against a 1,3,5-trichlorobenzene standard.³⁰

Analyses. EPR spectra were collected at X-band on a Bruker ELEXSYS E500 spectrometer equipped with a superhigh Q resonator and an Oxford ESR-900 helium-flow cryostat. Samples were sparged with N₂ and sonicated to remove any dissolved oxygen in solution. The reactions were frozen gradually in an ethanol/dry ice bath (195 K) and then transferred to liquid nitrogen. Data were collected at 7–8 K using 8 mW microwave power.

UV-vis spectra were recorded at 1 nm resolution on a Varian Cary50 using a 1.0 cm quartz cuvette. Kinetic measurements were taken every 30 s for 5 min and then every 60 s for 50 min afterward (60 min total). Baseline measurements were taken in either neat solvent or blank electrolyte solutions.

Electrochemical studies were performed on a Pine Instruments AFCBP1 bipotentiostat using a standard three-electrode setup. Reference and working electrodes were purchased from Bioanalytical Systems, Inc. unless otherwise noted. The basal plane graphite electrode (surface area 0.09 cm²) was built and cleaned prior to every experiment according to a literature procedure.⁵⁷ A platinum wire was used as a counter electrode and a silver wire as a pseudoreference. Prior to and after each set of CVs, ferrocene was used as an external standard (Fc/Fc⁺ = +0.690 vs NHE in MeCN) to calibrate the reference to NHE.

ASSOCIATED CONTENT

Supporting Information

The Supporting Information is available free of charge on the ACS Publications website at DOI: 10.1021/acs.organomet.6b00525.

Additional ¹H NMR and EPR spectra as well as electrochemical and DLS data (PDF)

AUTHOR INFORMATION

Corresponding Author

*E-mail: robert.crabtree@yale.edu.

Notes

The authors declare the following competing financial interest(s): D.L.H. and R.H.C. are currently submitting a patent that contains intellectual property described in this article.

ACKNOWLEDGMENTS

This research was supported by the Center for Catalytic Hydrocarbon Functionalization, No. DE-SC0001298 (D.L.H. and R.H.C.), an Energy Frontier Research Center funded by the U.S. Department of Energy. D.L.H. acknowledges support by the National Science Foundation Graduate Research Fellowship Program under Grant No. DGE-1122492 and the Yale Dox Summer Research Fellowship. DLS measurements were conducted in the Yale Facility for Light Scattering. We thank Prof. Gary Brudvig for productive discussions about EPR analysis.

REFERENCES

- Arndtsen, B. A.; Bergman, R. G.; Mobley, T. A.; Peterson, T. H. *Acc. Chem. Res.* **1995**, *28* (3), 154–162.
- Crabtree, R. H. *J. Organomet. Chem.* **2004**, *689* (24), 4083–4091.
- Activation and Functionalization of C-H Bonds*; Goldberg, K. I., Goldman, A. S., Eds.; American Chemical Society, 2004; Vol. 885.
- Bergman, R. G. *Nature* **2007**, *446* (7134), 391–393.
- Shilov, A. E.; Shul'pin, G. B. *Chem. Rev.* **1997**, *97* (8), 2879–2932.
- Tolman, W. B. *Activation of Small Molecules: Organometallic and Bioinorganic Perspectives*; John Wiley & Sons, Ltd, 2006.
- Dick, A. R.; Sanford, M. S. *Tetrahedron* **2006**, *62* (11), 2439–2463.
- Cavani, F.; Teles, J. H. *ChemSusChem* **2009**, *2* (6), 508–534.
- Chen, M. S.; White, M. C. *Science* **2007**, *318* (5851), 783–787.
- Gunay, A.; Theopold, K. H. *Chem. Rev.* **2010**, *110* (2), 1060–1081.
- Punniyamurthy, T.; Velusamy, S.; Iqbal, J. *Chem. Rev.* **2005**, *105* (6), 2329–2364.
- Shul'pin, G. B. *Catalysts* **2016**, *6* (4), 50.
- Zhou, M.; Crabtree, R. H. *Chem. Soc. Rev.* **2011**, *40* (4), 1875–1884.
- Periana, R. A.; Bhalla, G.; Tenn, W. J., III; Young, K. J. H.; Liu, X. Y.; Mironov, O.; Jones, C. J.; Ziatdinov, V. R. *J. Mol. Catal. A: Chem.* **2004**, *220* (1), 7–25.
- Tinberg, C. E.; Lippard, S. J. *Acc. Chem. Res.* **2011**, *44* (4), 280–288.
- Merckx, M.; Kopp, D. A.; Sazinsky, M. H.; Blazyk, J. L.; Müller, J.; Lippard, S. J. *Angew. Chem., Int. Ed.* **2001**, *40* (15), 2782–2807.
- Stone, K. L.; Borovik, A. S. *Curr. Opin. Chem. Biol.* **2009**, *13* (1), 114–118.
- Valentine, A.; Lippard, S. J. *Chem. Soc., Dalton Trans.* **1997**, 3925–3932.
- Karlin, K. D. *Science* **1993**, *261* (5122), 701–708.
- Que, L.; Tolman, W. B. *Nature* **2008**, *455* (7211), 333–340.
- McLain, J. L.; Lee, J.; Groves, J. T. In *Biomimetic Oxidations Catalyzed by Transition Metal Complexes*; Imperial College Press, 2000; pp 91–169.
- Baik, M.-H.; Newcomb, M.; Friesner, R. A.; Lippard, S. J. *Chem. Rev.* **2003**, *103* (6), 2385–2420.
- Costas, M.; Chen, K.; Que, L., Jr. *Coord. Chem. Rev.* **2000**, *200*–202, 517–544.
- Blackman, A. G.; Tolman, W. B. In *Metal-Oxo and Metal-Peroxo Species in Catalytic Oxidations*; Meunier, B., Ed.; Springer: Berlin, Heidelberg, 2000; pp 179–211.

- (25) Lewis, E. A.; Tolman, W. B. *Chem. Rev.* **2004**, *104* (2), 1047–1076.
- (26) Kamata, K.; Yonehara, K.; Nakagawa, Y.; Uehara, K.; Mizuno, N. *Nat. Chem.* **2010**, *2* (6), 478–483.
- (27) Shilov, A. E.; Shteinman, A. A. *Acc. Chem. Res.* **1999**, *32* (9), 763–771.
- (28) Zhou, M.; Hintermair, U.; Hashiguchi, B. G.; Parent, A. R.; Hashmi, S. M.; Elimelech, M.; Periana, R. A.; Brudvig, G. W.; Crabtree, R. H. *Organometallics* **2013**, *32*, 957–965.
- (29) Zhou, M.; Balcells, D.; Parent, A. R.; Crabtree, R. H.; Eisenstein, O. *ACS Catal.* **2011**, *2* (2), 208–218.
- (30) Zhou, M.; Schley, N. D.; Crabtree, R. H. *J. Am. Chem. Soc.* **2010**, *132* (36), 12550–12551.
- (31) Kawahara, R.; Fujita, K.; Yamaguchi, R. *J. Am. Chem. Soc.* **2012**, *134* (8), 3643–3646.
- (32) Hanasaka, F.; Fujita, K.; Yamaguchi, R. *Organometallics* **2004**, *23* (7), 1490–1492.
- (33) Burger, P.; Bergman, R. G. *J. Am. Chem. Soc.* **1993**, *115* (22), 10462–10463.
- (34) Hintermair, U.; Sheehan, S. W.; Parent, A. R.; Ess, D. H.; Richens, D. T.; Vaccaro, P. H.; Brudvig, G. W.; Crabtree, R. H. *J. Am. Chem. Soc.* **2013**, *135* (29), 10837–10851.
- (35) Yang, K. R.; Matula, A. J.; Kwon, G.; Hong, J.; Sheehan, S. W.; Thomsen, J. M.; Brudvig, G. W.; Crabtree, R. H.; Tiede, D. M.; Chen, L. X.; Batista, V. S. *J. Am. Chem. Soc.* **2016**, *138* (17), 5511–5514.
- (36) Shopov, D. Y.; Rudshteyn, B.; Campos, J.; Batista, V. S.; Crabtree, R. H.; Brudvig, G. W. *J. Am. Chem. Soc.* **2015**, *137* (22), 7243–7250.
- (37) Junge, H.; Marquet, N.; Kammer, A.; Denurra, S.; Bauer, M.; Wohlrab, S.; Gärtner, F.; Pohl, M.-M.; Spannenberg, A.; Gladiali, S.; Beller, M. *Chem. - Eur. J.* **2012**, *18* (40), 12749–12758.
- (38) Zuccaccia, C.; Bellachioma, G.; Bolaño, S.; Rocchigiani, L.; Savini, A.; Macchioni, A. *Eur. J. Inorg. Chem.* **2012**, *2012* (9), 1462–1468.
- (39) Savini, A.; Belanzoni, P.; Bellachioma, G.; Zuccaccia, C.; Zuccaccia, D.; Macchioni, A. *Green Chem.* **2011**, *13* (12), 3360–3374.
- (40) Zuccaccia, C.; Bellachioma, G.; Bortolini, O.; Bucci, A.; Savini, A.; Macchioni, A. *Chem. - Eur. J.* **2014**, *20* (12), 3446–3456.
- (41) Turlington, C. R.; Harrison, D. P.; White, P. S.; Brookhart, M.; Templeton, J. L. *Inorg. Chem.* **2013**, *52* (19), 11351–11360.
- (42) Materna, K. L.; Rudshteyn, B.; Brennan, B.; Kane, M.; Bloomfield, A.; Huang, D. L.; Shopov, D. Y.; Batista, V. S.; Crabtree, R. H.; Brudvig, G. W. *ACS Catal.* **2016**, *6*, 5371–5377.
- (43) Huang, D. L.; Beltrán-Suito, R.; Thomsen, J. M.; Hashmi, S. M.; Materna, K. L.; Sheehan, S. W.; Mercado, B. Q.; Brudvig, G. W.; Crabtree, R. H. *Inorg. Chem.* **2016**, *55* (5), 2427–2435.
- (44) Turlington, C. R.; White, P. S.; Brookhart, M.; Templeton, J. L. *J. Am. Chem. Soc.* **2014**, *136* (10), 3981–3994.
- (45) Turlington, C. R.; White, P. S.; Brookhart, M.; Templeton, J. L. *J. Organomet. Chem.* **2015**, *792*, 81–87.
- (46) Thomsen, J. M.; Sheehan, S. W.; Hashmi, S. M.; Campos, J.; Hintermair, U.; Crabtree, R. H.; Brudvig, G. W. *J. Am. Chem. Soc.* **2014**, *136* (39), 13826–13834.
- (47) Graeupner, J.; Brewster, T. P.; Blakemore, J. D.; Schley, N. D.; Thomsen, J. M.; Brudvig, G. W.; Hazari, N.; Crabtree, R. H. *Organometallics* **2012**, *31* (20), 7158–7164.
- (48) Brewster, T. P.; Blakemore, J. D.; Schley, N. D.; Incarvito, C. D.; Hazari, N.; Brudvig, G. W.; Crabtree, R. H. *Organometallics* **2011**, *30* (5), 965–973.
- (49) Diversi, P.; Fabrizi de Biani, F.; Ingrosso, G.; Laschi, F.; Lucherini, A.; Pinzino, C.; Zanello, P. *J. Organomet. Chem.* **1999**, *584* (1), 73–86.
- (50) Diversi, P.; Iacoponi, S.; Ingrosso, G.; Laschi, F.; Lucherini, A.; Pinzino, C.; Uccello-Barretta, G.; Zanello, P. *Organometallics* **1995**, *14* (7), 3275–3287.
- (51) Kawabata, K.; Nakano, M.; Tamura, H.; Matsubayashi, G. *Inorg. Chim. Acta* **2004**, *357* (15), 4373–4378.
- (52) Kaim, W.; Berger, S.; Greulich, S.; Reinhardt, R.; Fiedler, J. *J. Organomet. Chem.* **1999**, *582* (2), 153–159.
- (53) Parent, A. R.; Crabtree, R. H.; Brudvig, G. W. *Chem. Soc. Rev.* **2013**, *42* (6), 2247–2252.
- (54) Krow, G. R. In *Organic Reactions*; John Wiley & Sons, Inc., 2004.
- (55) Wong, Y.-L.; Yang, Q.; Zhou, Z.-Y.; Lee, H. K.; Mak, T. C. W.; Ng, D. K. P. *New J. Chem.* **2001**, *25* (2), 353–357.
- (56) Schley, N. D.; Blakemore, J. D.; Subbaiyan, N. K.; Incarvito, C. D.; D'Souza, F.; Crabtree, R. H.; Brudvig, G. W. *J. Am. Chem. Soc.* **2011**, *133* (27), 10473–10481.
- (57) Cady, C. W.; Shinopoulos, K. E.; Crabtree, R. H.; Brudvig, G. W. *Dalt. Trans.* **2010**, *39* (16), 3985–3989.